Available online at www.sciencedirect.com
SCIENCE DIRECT®
Lithos 75 (2004) 311–330
LITHOS
www.elsevier.com/locate/lithos

Abiogenic Fischer–Tropsch synthesis of hydrocarbons in alkaline igneous rocks; fluid inclusion, textural and isotopic evidence from the Lovozero complex, N.W. Russia

Joanna Potter[a,b,*], Andrew H. Rankin[b], Peter J. Treloar[b]

[a] *Institut für Mineralogie und Mineralische Rohstoffe, Technische Universität Clausthal, Adolph-Roemer Strasse, 2a 38678 Clausthal-Zellerfeld, Germany*

[b] *School of Earth Sciences and Geography, Kingston University, Penrhyn Road, Kingston-upon-Thames, Surrey KT1 2EE, UK*

Received 11 September 2003; accepted 10 March 2004
Available online 6 May 2004

Abstract

A detailed fluid inclusion study has been carried out on the hydrocarbon-bearing fluids found in the peralkaline complex, Lovozero. Petrographic, microthermometric, laser Raman and bulk gas data are presented and discussed in context with previously published data from Lovozero and similar hydrocarbon-bearing alkaline complexes in order to further understand the processes which have generated these hydrocarbons. CH_4-dominated inclusions have been identified in all Lovozero samples. They occur predominantly as secondary inclusions trapped along cleavage planes and healed fractures together with rare H_2O-dominant inclusions. They are consistently observed in close association with either arfvedsonite crystals, partially replaced by aegirine, aegirine crystals or areas of zeolitization. The majority of inclusions consist of a low-density fluid with CH_4 homogenisation temperatures between -25 and -120 °C. Those in near-surface hand specimens contain $CH_4 + H_2$ (up to 40 mol%) ± higher hydrocarbons. However, inclusions in borehole samples contain CH_4 + higher hydrocarbons ± H_2 indicating that, at depth, higher hydrocarbons are more likely to form. Estimated entrapment temperatures and pressures for these inclusions are 350 °C and 0.2–0.7 kbar. A population of high-density, liquid, CH_4-dominant inclusions have also been recorded, mainly in the borehole samples, homogenising between -78 and -99 °C. These consist of pure CH_4, trapped between 1.2 and 2.1 kbar and may represent an early CH_4-bearing fluid overprinted by the low-density population. The microthermometric and laser Raman data are in agreement with bulk gas data, which have recorded significant concentrations of H_2 and higher hydrocarbons up to C_6H_{12} in these samples. These data, combined with published isotopic data for the gases CH_4, C_2H_6, H_2, He and Ar indicate that these hydrocarbons have an abiogenic, crustal origin and were generated during postmagmatic, low temperature, alteration reactions of the mineral assemblage. This would suggest that these data favour a model for formation of hydrocarbons through Fischer–Tropsch type reactions involving an early CO_2-rich fluid and H_2 derived from alteration reactions. This is in contrast to the late-magmatic model suggested for the formation of hydrocarbons in the similar peralkaline intrusion, Ilímaussaq, at temperatures between 400 and 500 °C.

Keywords: Abiogenic; Hydrocarbons; Fischer–Tropsch synthesis; Igneous

* Corresponding author. Tel.: +49-5323-723670; fax: +49-5323-723737.
E-mail address: joanna.potter@tu-clausthal.de (J. Potter).

0024-4937/$ - see front matter © 2004 Elsevier B.V. All rights reserved.
doi:10.1016/j.lithos.2004.03.003

1. Introduction

Hydrocarbons interpreted as generated by abiogenic processes have been reported from a number of igneous terranes, in particular, from ultrabasic and peralkaline igneous complexes (see review by Potter and Konnerup-Madsen, 2003). A number of potential origins have been proposed for these hydrocarbons. These include a primary mantle origin (e.g., Gold, 1979), a late-magmatic origin (e.g., Karzhavin and Vendillo, 1970; Konnerup-Madsen et al., 1985; Kogarko et al., 1987), and a postmagmatic origin (e.g., Sherwood-Lollar et al., 1993; Salvi and Williams-Jones, 1997; Potter et al., 1998). The most recent data on these abiogenic hydrocarbons indicate that a primary mantle origin is unlikely. However, there are abundant analytical data that apparently support each of the late-magmatic and postmagmatic models. In this paper, a detailed fluid inclusion, petrographic and gas study on the fluids hosted in the Lovozero complex of northwest Russia is presented. These data, along with previously published data from similar complexes (e.g., Khibina and Ilímaussaq; Potter et al., 1998; Konnerup-Madsen et al., 1979) are used here to test and discuss both models and to provide a more detailed insight into the mechanisms involved in generating abiogenic hydrocarbons, not only in alkaline igneous rocks but in other igneous terranes as well.

2. Geological setting and petrology of samples

The Lovozero pluton is the second largest alkaline intrusion in the 100,000 km^2 Kola Alkaline Province of northwest Russia, the largest being the nearby Khibina pluton (Fig. 1a). Lovozero is located in the centre of the Kola Peninsula and is spatially related to the Kontozero–Khibina graben, a deep NW–SE trending Palaeozoic fault (Fig. 1a). The reactivation of this, and other, faults in the mid to late Devonian accompanied the production and emplacement of large volumes of alkaline magmas in the province (Dudkin and Mitrofanov, 1994).

The Lovozero pluton is a laccolithic, layered complex with a surface area of 650 km^2 (Fig. 1b). Rb–Sr whole rock data give ages between 371.6 ±20.3 and 361.7 ± 1.1 Ma (Kramm et al., 1993). The complex consists mainly of nepheline syenites, urtites and lujavrites. The lujavrites host large loparite deposits, which are rich in the rare earth elements Ta and Nb. The geology of the complex has been described extensively by Gerasimovsky et al. (1968) and summarised by Kogarko et al. (1995).

Table 1 shows a list of the main rock types analysed in this study, their mineral assemblages and peralkalinity index (PI). Peralkalinity was calculated using whole-rock bulk geochemical data (Potter, 2000) as defined by Sørensen (1997). The geochemical data are available on request. The agpaitic nature of the samples was determined mineralogically, as discussed by Sørensen (1997). The rare agpaitic minerals mentioned in this paper are also listed in Table 1. A detailed description of the petrology of these samples is available in Potter (2000).

The Lovozero samples are mineralogically and geochemically peralkaline and agpaitic in nature (Table 1). The urtites with the lowest PI (~ 1.04) contain arfvedsonite, titanite and sodalite indicating a low agpaicity. The more peralkaline urtites (PI = ~ 1.14) contain the rare agpaitic Na–Ti–Zr-silicates lamprophyllite, lomonosovite and penkvilsikite. The increase in peralkalinity in the foyaites (PI = ~ 1.25) coincides with the disappearance of magnetite and an increase in aegirine content together with the appearance of rare agpaitic Na silicates such as bornemanite. The juvites contain abundant loparite and eudialyte indicating they are highly agpaitic. Abundant eudialyte and aegirine are also present in the highly peralkaline lujavrites and eudialyte–lujavrites (PI = 1.3–1.5), as well as significant contents of rare Na silicates including murmanite, lovozerite, vlasovite and chkalovite indicating a hyperagpaitic nature. Arfvedsonite is commonly observed partially replaced by aegirine, particularly in the urtites.

3. Methodology

A total of 17 samples from the variety of rock suites in the Lovozero complex were selected for fluid inclusion analysis from a preliminary screening of approximately 40 typical rock types. Samples were supplied from two sources; near-surface hand specimens stored at the Kola Science Centre, Russia, and borehole samples stored at the Natural History Museum, UK. These samples were selected on the basis of the

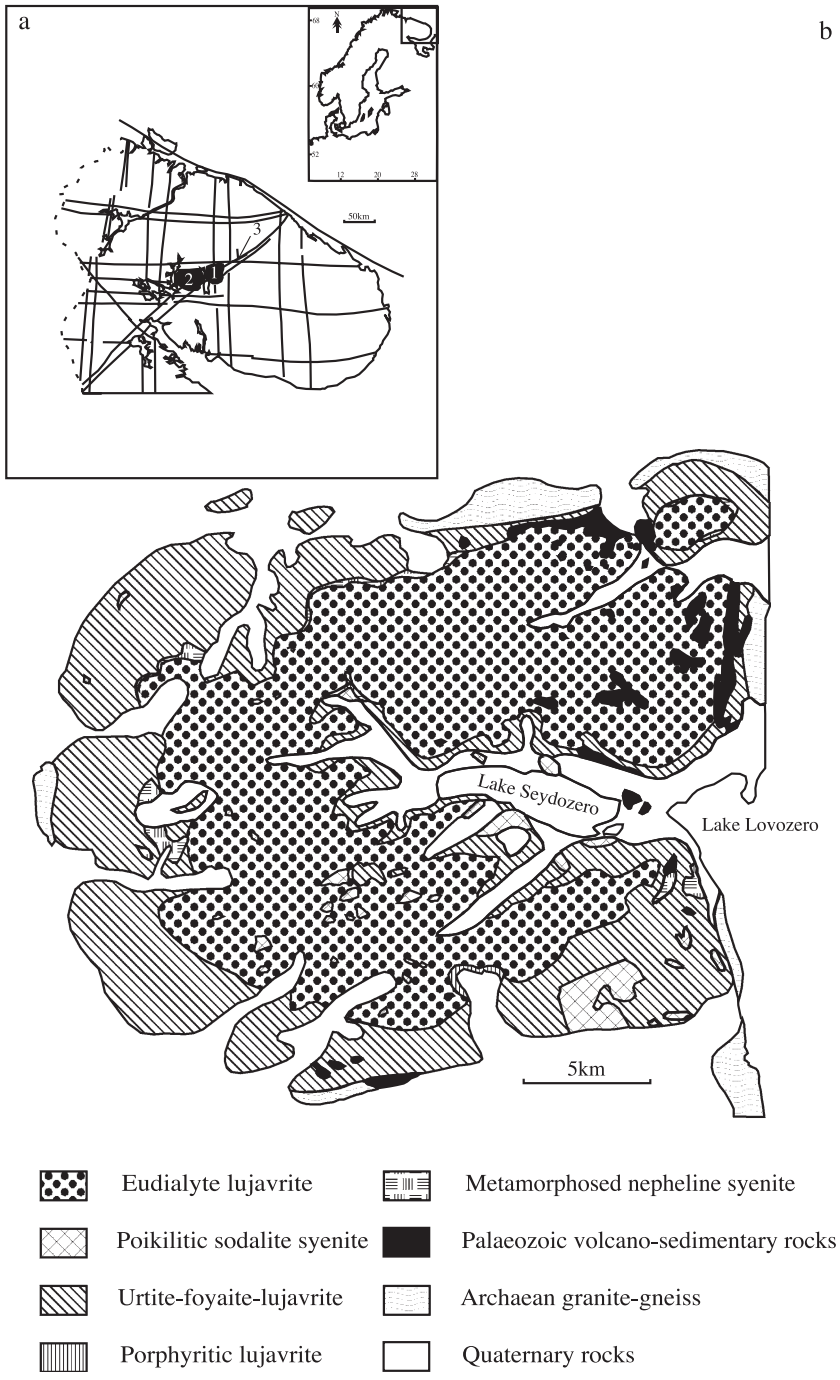

Fig. 1. (a) A locality map of the Kola Alkaline Province showing the main structural fault zones and locality of the major alkaline complexes Lovozero (1) and Khibina (2) located in the Khibina–Kontozero graben (3). (b) A geological map of the Lovozero intrusion. Based on Kogarko et al. (1995) and Dudkin and Mitrofanov (1994).

Table 1
The main rock types for each intrusion and their mineralogy with sample numbers used in the fluid inclusion study

Rock type	Main minerals	Accessories	Sample numbers	PI (Na + K)/Al
Urtite	Ne, Aeg, Arf, Ab	Alk Fs, Mag, Sdl, Ttn, Ntr, Anl, Lop, Lamp, K-gmel, Lom, Penk	UG-54, L 121	1.04–1.14
Foyaite	Ab, Ne, Aeg	Alk Fs, Eud, Sdl, Arf, Ap, Born, Ttn, Ccn, Ntr, Anl, Lop	L 34, L 76, L 98, L 139, TS-18-2, 727-9	1.21–1.25
Lujavrite	Ab, Ne, Aeg	Alk Fs, Eud, Sdl, Aug, Arf, Ttn, Lop, Ntr, Ccn, Anl, Pyr, Mur, Vlas	L 21, L 135, L 228, L 276, 146-6	1.28–1.40
Eudialyte lujavrite	Ab, Ne, Aeg, Eud	Alk Fs, Sdl, Arf, Ntr, Anl, Lov, Chk	L-16-11, L 83, L167	1.24–1.48
Loparite juvite	Ne, Ab, Aeg, Lop	Alk Fs, Eud, Sdl, Anl	L-16-19	1.32

Born: bornemanite ($Na_7BaTi_2NbSi_4PO_{21}F$); Chk: chkalovite ($Na_2BeSi_3O_8$); K-gmel: K-gmelinite ($KAlSi_2O_6{\cdot}3H_2O$); Lamp: lamprophyllite ($Na_6Sr_3FeTi_6Si_8O_{34}F_2$); Lom: lomonosovite ($Na_2Ti_2Si_2O_9{\cdot}Na_3PO_4$); Lop: loparite ($NaCeTi_2O_6$); Lov: lovozerite ($H_3Na_3CaZrSi_6O_{18}{\cdot}H_2O$); Mur: murmanite ($Na_3Ti_4Si_4O_{17}F{\cdot}5H_2O$); Penk: penkvilsikite ($Na_2TiSi_4O_{11}{\cdot}2H_2O$); Vlas: vlasovite ($Na_2ZrSi_4O_{11}$).
All other abbreviations, refer to Kretz (1983).

abundance of suitable host minerals, such as nepheline, eudialyte and sodalite, and the number of fluid inclusions present. For each sample, polished thin sections were prepared for microprobe analysis and double-polished 100–150 μm fluid inclusion wafers for microthermometric and laser Raman microprobe analysis. The petrographic characteristics and textural relationships of the fluid inclusion arrays (i.e., size, shape, distribution and abundance) were recorded in order to determine fluid inclusion populations and their timing of entrapment, following established criteria (Roedder, 1984; Van den Kerkhof and Hein, 2001).

Fluid inclusion microthermometric analysis was carried out using a Linkam THMS600 low-temperature, heating–freezing stage attached to a Nikon microscope. Measurements were carried out over the temperature range −196 to +600 °C following the methodology and procedures of Shepherd et al. (1985). Stage calibrations were carried out regularly using pure substances with known melting points (Roedder, 1984) and synthetic fluid inclusion standards. All measurements reported in this paper are accurate to within ±0.5 °C from −100 to 100 °C and to within ±1 °C from −196 to −100 °C and from 100 to 600 °C. Wherever possible, the following measurements were made: temperatures of homogenisation of the liquid and vapour components of CH_4 (Th_{CH_4}), first ice melting temperature of aqueous inclusions (Te), last ice melting temperature of aqueous inclusions (Tm-ice), clathrate melting temperature of aqueous inclusions (Tm-clath) and total homogenisation temperatures to liquid or vapour (T-t-L/V). Methane phase behaviour is described according to the criteria of Van den Kerkhof (1988) and Van den Kerkhof and Thiéry (2001).

An Oxford Instruments, ISIS energy-dispersive system mounted on a JEOL 6300 scanning electron microscope was used to analyse mineral compositions and identify any discrete mineral phases relating to alteration of the mineral assemblages.

A confocal, multichannel Renishaw laser Raman microprobe (RM 1000) with an argon ion laser (514.5 nm) and thermoelectrically cooled CCD detector system was used to determine fluid inclusion gas compositions. The laser Raman system was attached to an Olympus microscope with lens magnification up to ×80 enabling analysis of areas ≤4 μm^2 in size. The microprobe was calibrated regularly using a silicon standard to check and correct for any drift. Reported peak positions are accurate to within ±1 cm^{-1} Raman shift. Run times for spectra were approximately 30 s for an extended spectrum from 100 to 5000 cm^{-1}. Mole percentages of gas mixtures were calculated using the criteria described by Burke (2001), using reported Raman scattering cross-sections (σ) for the appropriate excitation wavelength.

Two bulk gas methods were used to analyse the chemical composition of volatiles released during the heating and crushing of whole rock samples. Gas chromatographic analyses were carried out at the Kola Science Centre, Russia based on methods described by Ikorski and Voloshin (1982) and Ikorski et al. (1992). These analyses were done using a PE F-30 gas-chromatograph with a 5-Å molecular sieve packed column and Ar (5.0) carrier gas to separate He, H_2, O_2, N_2, CH_4, CO and C_2H_6 and a spherocrom packed column with

He (5.0) carrier gas to separate out CH_4, CO_2 and C_2–C_5 gas species. The gases were extracted from ~1 g of whole-rock sample by crushing in a sealed vacuum ball mill before subsequent release into the gas carrier stream. Gases present were detected by a flame ionisation detector (FID). Further comparative data were obtained from mass-spectrometric analyses at Fluid Inclusion Technologies (Oklahoma, USA), using a

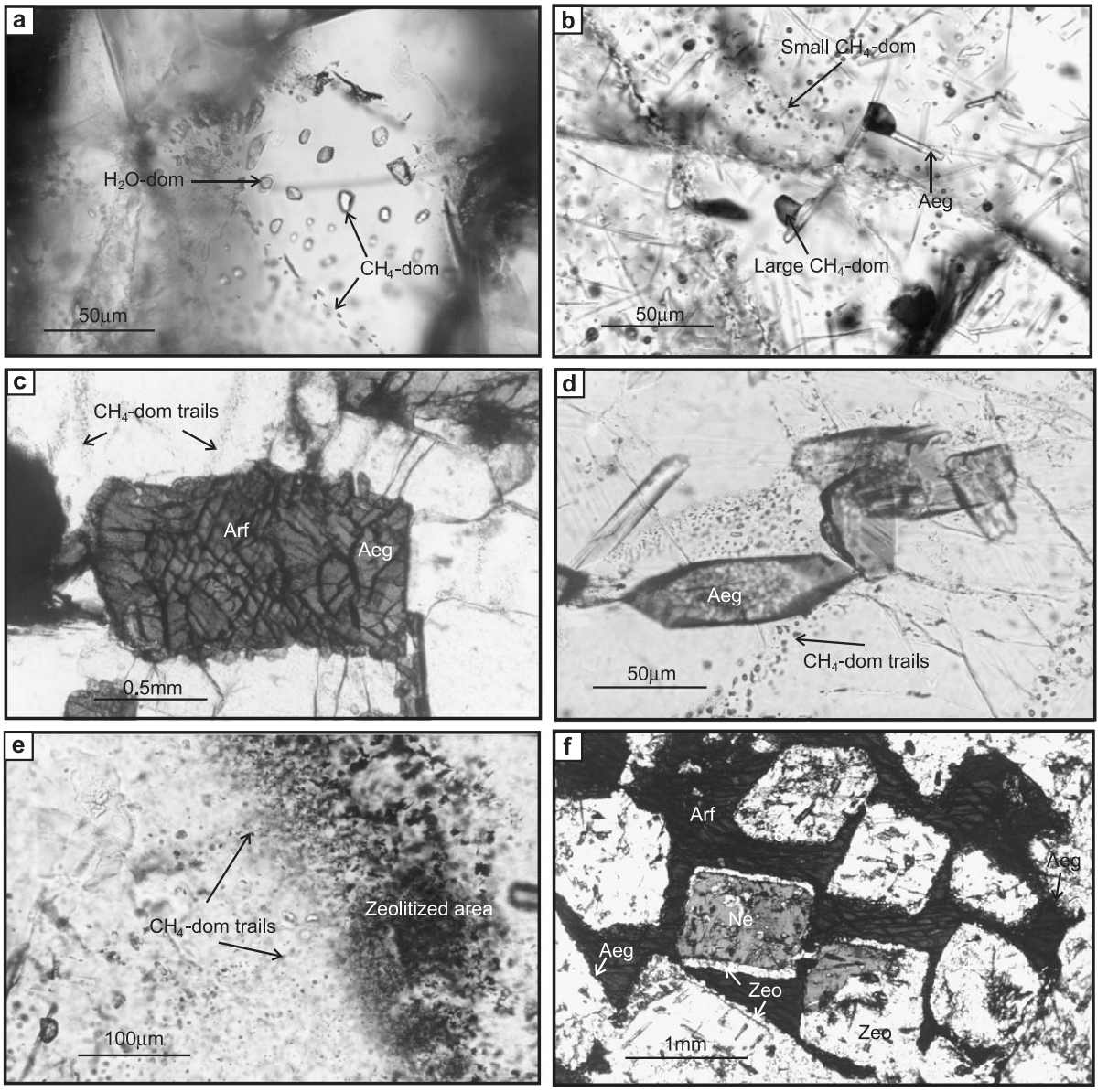

Fig. 2. The distribution of inclusions in Lovozero. (a) H_2O-dominant inclusions in trails with CH_4-dominant inclusions in eudialyte from eudialyte lujavrites. (b) Large CH_4-dominant inclusions attached to aegirine microlites together with trails of smaller inclusions in nepheline in lujavrites. (c) Trails of CH_4-dominant inclusions extending out into the nepheline host from arfvedsonite crystals, partially replaced by aegirine in urtites. (d) CH_4-dominant inclusions concentrated around aegirine crystals in eudialyte lujavrites. (e) Trails of CH_4-dominant inclusions extending out into the nepheline host from areas of zeolitization in urtites. (f) Nepheline chadocrysts in arfvedsonite with reaction rims of aegirine and zeolite (e.g., analcite or natrolite) in urtites.

Table 2
Summary of microthermometric and laser Raman data for fluid inclusions in Lovozero

Rock type	Sample	Inc Type	*N*	Host	Th_{CH_4}		Volatiles detected by L–R
Luj	L 21	CH_4	14	Ne	−81.5 to −90.1	V	na
Foy	L 34	CH_4	5	Ne	−79.5 to −85.2	V	na
	L 34	CH_4	11	Ne	−77.8 to −87.7	L	na
Foy	L 76	CH_4	9	Ne	−75.9 to −85.2	V	$CH_4 \pm$ HHC
	L 76	CH_4	1	Alk Fs	−84.0	V	$CH_4 \pm$ HHC
	L 76	CH_4	31	Ne	−80.9 to −89.7	L	$CH_4 \pm$ HHC
	L 76	CH_4	8	Alk Fs	−80.3 to −83.5	L	$CH_4 \pm$ HHC
Eud–luj	L 83	CH_4	11	Ne	−80.2 to −89.1	V	$CH_4 \pm$ HHC
	L 83	CH_4	14	Ne	−82.2 to −84.4	L	$CH_4 \pm$ HHC
Foy	L 98	CH_4	12	Ne	−64.7 to −86.2	V	na
	L 98	CH_4	9	Alk Fs	−50.2 to −83.6	V	na
	L 98	CH_4	10	Ne	−77.7 to −99.3	L	na
	L 98	CH_4	2	Alk Fs	−77.7 to −80.5	L	na
	L 98	CH_4	1	Ap	−99.3	L	na
Urt	L 121	CH_4	7	Ne	−81 to −88.3	V	na
Luj	L 135	CH_4	61	Ne	−25.1 to −106.9	V	$CH_4 \pm$ HHC
	L 135	CH_4	10	Eud	−81.5 to −90.5	V	$CH_4 \pm$ HHC
	L 135	CH_4	9	Alk Fs	−43.4 to −89.3	V	$CH_4 \pm$ HHC
	L 135	CH_4	9	Sdl	−81.8 to −88.2	V	$CH_4 \pm$ HHC
	L 135	CH_4	14	Ne	−80.9 to −83.3	L	$CH_4 \pm$ HHC
	L 135	CH_4	2	Eud	−81.6 to −82.3	L	$CH_4 \pm$ HHC
	L 135	H_2O	2	Ne	[a]		na
Foy	L 139	CH_4	3	Ne	−80.9 to −84.1	L	na
	L 139	CH_4	1	Ne	−81.1[b]	V	na
Eud–luj	L 167	CH_4	23	Ne	−27.8 to −110.3[b]	V	$CH_4 \pm H_2 \pm H_2O \pm$ HHC
	L 167	CH_4	9	Eud	−84.8 to −103.6[b]	V	$CH_4 \pm H_2 \pm H_2O \pm$ HHC
	L 167	H_2O	4	Ne	[a]		na
Luj	L 228	CH_4	45	Ne	−78.2 to −119.5[b]	V	$CH_4 \pm H_2 \pm H_2O \pm$ HHC
	L 228	CH_4	2	Ne	−84.1 to −86.1	L	$CH_4 \pm H_2 \pm H_2O \pm$ HHC
Luj	L 276	CH_4	5	Ne	−82.5 to −98.8	V	$CH_4 \pm H_2O \pm$ HHC
	L 276	CH_4	5	Eud	−80.9 to −87.2	V	$CH_4 \pm H_2O \pm$ HHC
Foy	727-9	CH_4	26	Ne	−67.6 to −85.5	V	$CH_4 \pm$ HHC
	727-9	CH_4	8	Eud	−75.7 to −83.0	V	$CH_4 \pm$ HHC
	727-9	CH_4	2	Alk Fs	−80.7 to −80.8	V	$CH_4 \pm$ HHC
	727-9	CH_4	2	Ap	−71.9 to −85.5	V	$CH_4 \pm$ HHC
	727-9	CH_4	4	Ne	−80.1 to −88.1	L	$CH_4 \pm$ HHC
Urt	UG-54	CH_4	6	Ne	−84.4 to −115.0[b]	V	$CH_4 \pm H_2 \pm H_2O \pm$ HHC
	UG-54	CH_4	17	Ne	−89.8 to −95.4	Cr	$CH_4 \pm H_2 \pm H_2O \pm$ HHC
	UG-54	CH_4	5	Eud	−89.8 to −95.6[b]	V	$CH_4 \pm H_2 \pm H_2O \pm$ HHC
	UG-54	CH_4	1	Ne	−89.7	L	$CH_4 \pm H_2 \pm H_2O \pm$ HHC
	UG-54	CH_4	1	Eud	−90.4	L	$CH_4 \pm H_2 \pm H_2O \pm$ HHC
Foy	TS-18-2	CH_4	22	Ne	−67.4 to −90.2	V	na
	TS-18-2	CH_4	3	Eud	−77 to −81.5	V	na
	TS-18-2	CH_4	7	Alk Fs	−80.0 to −90.2	V	na
Eud–luj	L-16-11	CH_4	47	Ne	−62.5 to −109.5	V	$CH_4 \pm H_2 \pm H_2O \pm$ HHC
	L-16-11	CH_4	2	Alk Fs	−81.2 to −86.9	V	$CH_4 \pm H_2 \pm H_2O \pm$ HHC
	L-16-11	CH_4	10	Ne	−78.1 to −83.8	L	$CH_4 \pm H_2 \pm H_2O \pm$ HHC
Lop–juv	L-16-19	CH_4	15	Ne	−77.7 to −105.2	V	na
	L-16-19	CH_4	3	Aeg	−84.5 to −92.1	V	na
Luj	146-6	CH_4	4	Ne	−84.0 to −92.2	V	na
	146-6	CH_4	3	Ne	−82.2 to −83.0	L	na

quadrupole mass-spectrometer. Samples were selected based on observed fluid inclusion populations and sent for analysis. These samples (~ 1–3 g) were placed in a vacuum oven, baked and then crushed at ultrahigh vacuum to release the volatiles that were then transferred into the quadrupole mass-spectrometer (refer to FIT website for additional details).

PVTX modelling of fluid inclusion data enabled calculation of fluid densities, salinities and volumetric properties. Calculations utilised the appropriate microthermometric data and equations of state (EoS) using software developed by Bakker (2001). The EoS used were based on those of Duan et al. (1992, 1995, 1996), Soave (1972) and Thiéry et al. (1994) for gas mixtures of CH_4–H_2–C_2H_6. Other data used in determining compositions and trapping conditions of the different fluid types include data for the H_2O–CH_4 system (Zhang and Frantz, 1992), the CH_4–C_2H_6 system (Olds, 1953) and the H_2O–NaCl system (Brown and Lamb, 1989).

4. Analytical data

4.1. Fluid inclusion types and distribution

Two fluid inclusion compositional types have been identified in the Lovozero samples: CH_4-dominant and H_2O-dominant inclusions. The CH_4-dominant inclusions are the most abundant and are present in all the samples analysed. H_2O-dominant inclusions are rare and have been identified in only two samples in which they occur as ~ 10 μm, rounded, biphase (L + V) inclusions in trails together with the CH_4-dominant inclusions in nepheline, eudialyte or sodalite (Fig. 2a). CH_4-dominant inclusions occur as either large, 10–30 μm, rounded monophase inclusions or as smaller, 5–10 μm, monophase inclusions in secondary trails that cross-cut grain boundaries (Fig. 2b). These two morphological types occur together along cleavage planes in nepheline and feldspar. Sinuous trails of small CH_4-dominant inclusions occupy healed fractures in eudialyte and sodalite. These CH_4-dominant inclusions are almost always found associated with arfvedsonite, aegirine and zeolites. The large inclusions are commonly attached to aegirine microlites in nepheline (Fig. 2b). The small inclusions often occur in secondary trails that extend outward from arfvedsonite crystals partially replaced by aegirine, into the nepheline host (Fig. 2c). Alternatively, secondary trails of CH_4-dominant inclusions can be found in close association with aegirine crystals (Fig. 2d), or extending out from areas of zeolitization (Fig. 2e). A petrographic plate of an urtite containing abundant CH_4-dominant inclusions is shown in Fig. 1f, demonstrating the mineral phase associations. A large, poikilitic arfvedsonite crystal engulfs euhedral nepheline chadocrysts. Reaction rims of aegirine and zeolites can be observed between the arfvedsonite and nepheline.

4.2. Microthermometric data

Microthermometric analysis was carried out on 537 inclusions from 17 samples. These data are summarised in Table 2. Both the large and small CH_4-dominant inclusions show H1 behaviour on heating/cooling (i.e., separation into a liquid and vapour phase at low temperatures; Van den Kerkhof and Thiéry, 2001) with a wide range of CH_4 homogenisation temperatures (Th_{CH_4}) between −25 and −120 °C, predominantly to vapour (~ 75%; Fig. 3). Inclusions in certain samples (UG-54, L 167, L 228) proved unresponsive (~ 15% of the population) with no observable phase changes during cooling down to −196 °C. These inclusions were found in the same trails as those showing low Th_{CH_4} (−90 to −120 °C). These unresponsive inclusions will henceforth be classified as inclusions displaying H0 behaviour (i.e., no observable phase changes down to −196 °C). The majority of the

Notes to Table 2:
N: number of fluid inclusions recorded; Th_{CH_4}: temperature of homogenisation of CH_4.
Eud–luj: eudialyte lujavrite; Foy—foyaite; Lop–juv—loparite juvite; Luj—lujavrite; Urt—Urtite; Ne—nepheline; Eud—eudialyte; Sdl—sodalite; Alk Fs—alkali feldspar.
HHC: higher hydrocarbons; na: not analysed. L-16-19 and 146-6 results reported in Potter et al. (1998).
[a] H_2O data: temperature of melting of clathrate = 11.0–15.8 °C, last ice melting temperature = −5.3 to −5.8 °C, temperature of total homogenisation (V) = 290.7–354.6 °C.
[b] H0 inclusions.

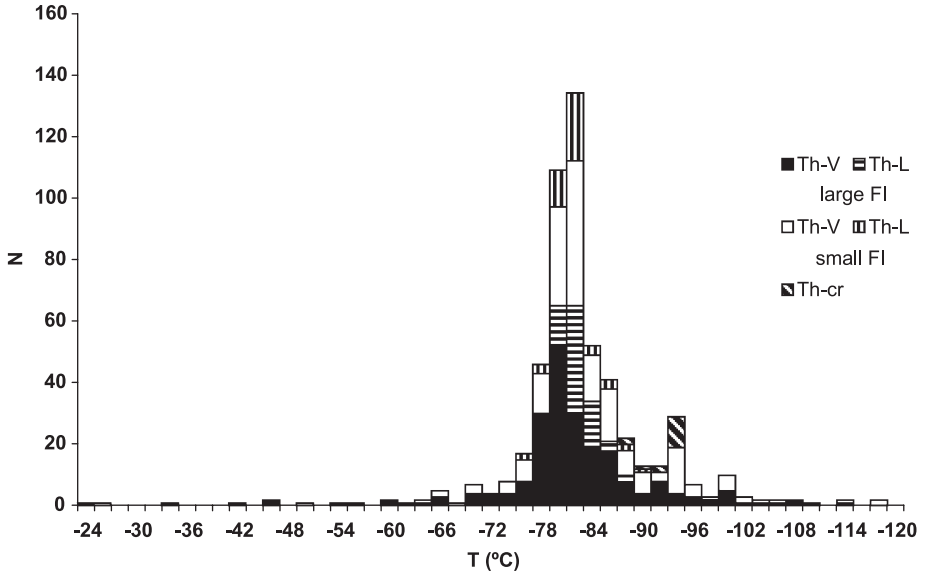

Fig. 3. The range of CH_4 homogenisation temperatures to vapour (Th-V), liquid (Th-L) or critical (Th-cr) phases for small and large CH_4-dominant inclusions in Lovozero.

inclusions, however, homogenised between −62 and −90 °C (Fig. 3), most of which have values of Th_{CH_4} that cluster around the critical temperature of pure CH_4 (Tcr_{CH_4} = −82 °C). The rare H_2O-dominant inclusions have clathrate melting temperatures of 11 to 15.8 °C, inferred to be a CH_4 rather than a CO_2 clathrate as it has a melting temperature of >10 °C. Total homogenisation temperatures were to vapour, between 291 and 355 °C. Last ice melting temperatures were between −5.3 and −5.8 °C, equal to 8.2–8.8 equiv. wt.% NaCl.

4.3. Laser Raman data

Those inclusion arrays that showed variable Th_{CH_4} values were subsequently analysed by laser Raman spectroscopy in order to determine if any volatiles other than CH_4 and H_2O were present. Fig. 4 shows some representative spectra from these inclusions. All inclusions show a CH_4 peak between 2911 and 2915 cm^{-1} (Fig. 4). In inclusions showing low Th_{CH_4} (< −88 °C), or displaying H0 behaviour (i.e., samples L 228 and UG-54), it is apparent that, in addition to CH_4, H_2 is also present, as evident from the peak at 4152 cm^{-1} (Fig. 4a, b). Calculations show that these inclusions can contain up to 40 mol% H_2. Higher hydrocarbons are also present as evident from the small peaks for C_2H_6 (2954 cm^{-1}) and C_3H_8 (2890 cm^{-1}) rising above the background in the vicinity of the CH_4 peak (Fig. 4a). In inclusions showing high Th_{CH_4} (> −80 °C), the background becomes more elevated around the CH_4 peak and C_2H_6, C_3H_8 and trace amounts of H_2O can be identified (Fig. 4c). A broad fluorescent shoulder may be present at wavelengths above 3000 cm^{-1}, indicating that more complex hydrocarbons are also present (Fig. 4d). The volatiles detected in each sample studied are shown in Table 2 along with the corresponding microthermometric data.

4.4. Bulk gas data

Whole-rock gas chromatographic data are shown in Table 3 for Lovozero samples obtained from the Kola Science Centre. The gas-chromatographic method is effective for quantifying He and CH_4 concentrations. However, the extraction of gases by crushing in a vacuum ball mill has limitations. H_2 can be generated from mineral–H_2O interactions and atmospheric contamination and/or N_2 generated from trapped NH_4^+ ions in mineral lattices during crushing can give inaccurately high concentrations for these gases in the results. Adsorption effects can also be high for gases such as CO, CO_2 and higher alkanes; therefore, these trace components may escape detection (Nivin, personal communication; Salvi and Williams-Jones, 2003).

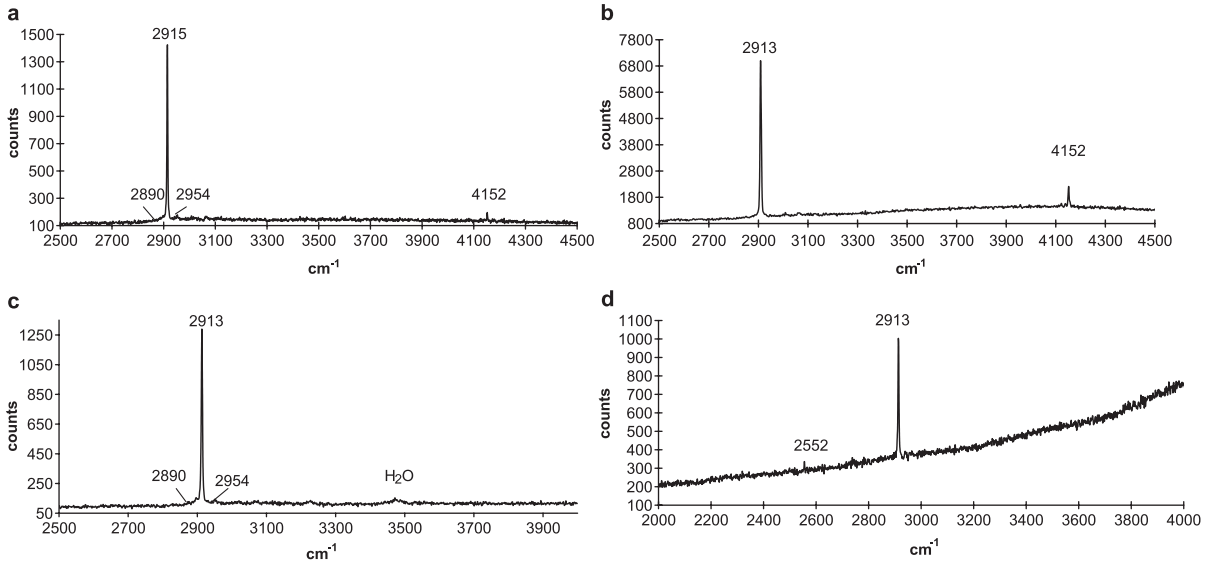

Fig. 4. Representative laser Raman spectra for CH_4-dominant inclusions in Lovozero samples. (a) A spectra showing peaks for a gas mixture of CH_4 (88 mol%), C_2H_6 (1 mol%), H_2 (11 mol%) and trace C_3H_8 in L 228. (b) Spectra showing peaks for CH_4 (70 mol%) and H_2 (30 mol%) in inclusions showing low CH_4 homogenisation temperatures in UG-54. (c) Spectra showing CH_4 with trace amounts of C_2H_6, C_3H_8 and H_2O in L-16-11. (d) A typical spectra for inclusions in L 167 with high Th_{CH_4} showing a fluorescent shoulder at high wavelengths (the small sharp peak at 2552 cm^{-1} is from the sodalite host).

Results show that total gas concentrations are moderate, with up to 28 cm^3/kg recorded, with the highest concentrations in the urtite. The dominant gas species present is CH_4 (up to 89 vol.%). Other significant gases are H_2 (up to 35 vol.%) and C_2H_6 (up to 7 vol.%). The urtite contains the highest concentrations of H_2 at 8 cm^3/kg. These results are similar to those reported by Nivin et al. (2001) for free gases (CH_4—60 vol.%, H_2—35 vol.%, C_2H_6—3.2 vol.%, He—2 vol.%) and inclusion gases (CH_4—76 vol.%, H_2—20 vol.%, C_2H_6—5 vol.%, He—0.07 vol.%) at Lovozero. No CO_2 or C_3–C_5 hydrocarbons have been detected by this method but this may be due to the limitations described above. The N_2 detected (up to 6.5 vol.%) has not been identified in fluid inclusions during laser Raman investigations. Therefore, this N_2 may be from contamina-

Table 3
Bulk gas-chromatographic data from Lovozero samples in vol.% and cm^3/kg

Sample	Rock	CH_4 (vol.%)	C_2H_6 (vol.%)	H_2 (vol.%)	CO_2 (vol.%)	N_2 (vol.%)	He (vol.%)	
L-16-11	Eud Lujavrite	87.17	2.86	5.13	0.00	4.84	0.00	
L-16-19	Lop Juvite	62.71	4.40	25.92	0.00	6.48	0.50	
TS-8-2	Lujavrite	65.30	6.91	24.66	0.00	3.12	0.02	
146-6	Lujavrite	52.06	6.44	35.24	0.00	5.72	0.52	
727-9	Foyaite	89.43	1.92	4.14	0.00	4.51	0.00	
UG-54	Urtite	62.72	6.80	27.76	0.00	2.69	0.02	
Sample	Rock	CH_4 (cm^3/kg)	C_2H_6 (cm^3/kg)	H_2 (cm^3/kg)	CO_2 (cm^3/kg)	N_2 (cm^3/kg)	He (cm^3/kg)	Total (cm^3/kg)
L-16-11	Eud Lujavrite	20.72	0.68	1.22	0.00	1.15	0.0010	23.77
L-16-19	Lop Juvite	5.13	0.36	2.12	0.00	0.53	0.0410	8.18
TS-8-2	Lujavrite	4.82	0.51	1.82	0.00	0.23	0.0016	7.38
146-6	Lujavrite	2.91	0.36	1.97	0.00	0.32	0.0290	5.59
727-9	Foyaite	23.78	0.51	1.10	0.00	1.20	0.0015	26.59
UG-54	Urtite	17.71	1.92	7.84	0.00	0.76	0.0058	28.24

tion effects, either from the atmosphere or from NH_4^+ released from feldspars.

The mass-spectrometric technique is more sensitive and can detect a whole range of volatile species in one run. However, quantitative analysis of gas concentrations is not possible with this procedure due to overloading of the detectors with the dominant gas species and problems calculating the contribution of H_2O and separating and resolving the various hydrocarbon ionised fragments detected (FIT website; Salvi and Williams-Jones, 2003). Therefore, this technique can only be used as a comparative tool by observing the relative abundances of gas species present between samples in conjunction with other data. Fig. 5 shows representative quadrupole mass spectrometry data for different rock types from Lovozero. Gaseous species are identified from their mass/charge ratio (m/z). The dominant gas species present in all rock types is CH_4. Higher hydrocarbons up to C_5 are also present in all samples, the response decreasing with increasing carbon number (Cn). Significant concentrations (i.e., $>10^3$ mV response) of C_6H_{14} were also found in the loparite juvite. Highest gas concentrations were found in the foyaites and lujavrites (Fig. 5b, c). Highest H_2 concentrations were recorded in the uritites, lujavrites and eudialyte lujavrites (Fig. 5a, c, d, e). These data are in good agreement with the gas-chromatographic data (Table 3) and the fluid inclusion observations (Table 2).

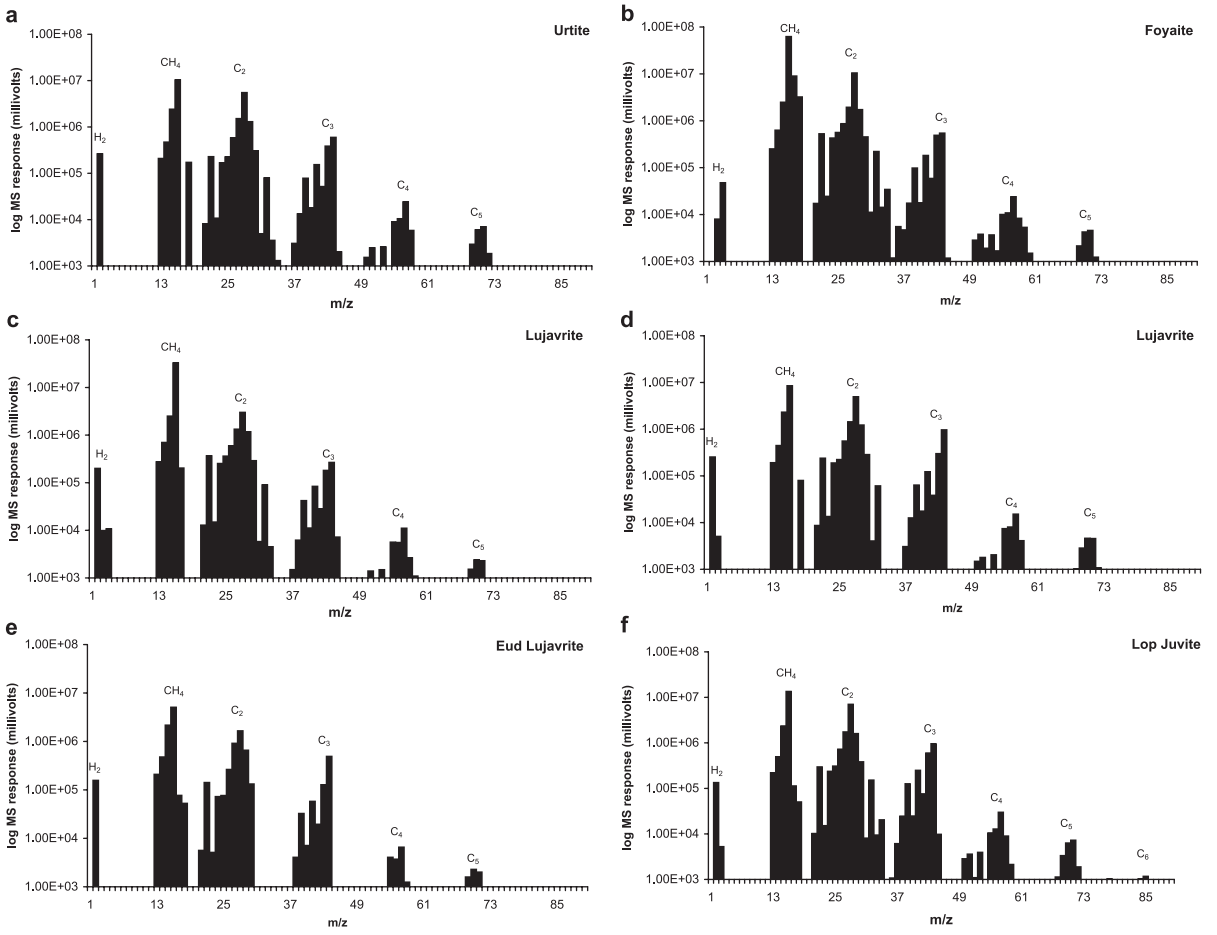

Fig. 5. Examples of quadrupole mass spectrometer analyses for the different rock types at Lovozero. m/z: mass/charge ratios ranging from 1 to 90. $CH_4 = 15-16$, $C_2H_6 = 28-30$, $C_3H_8 = 40-44$, $C_4H_{10} = 54-58$, $C_5H_{12} = 68-71$, $C_6H_{14} = 84-86$. (a) UG-54; (b) 727-9; (c) L 135; (d) 146-6; (e) L 167; (f) L-16-19.

5. Summary and interpretation of results

The petrographic distribution of the CH_4-dominant and H_2O-dominant inclusions implies that they were trapped as secondary inclusions. The textural relations would suggest that the inclusions were trapped during postmagmatic alteration of the early mineral assemblage to aegirine and zeolites. The rarity of H_2O-dominant inclusions in Lovozero samples and the coexistence of these inclusions in the same trails as the CH_4-dominant inclusions implies coeval, immiscible trapping of these two fluids, at or below the CH_4–H_2O solvus at ~ 350 °C (Zhang and Frantz, 1992), supporting a postmagmatic origin for these fluids. This is also indicated by the microthermometric data for the H_2O-dominant inclusions that homogenise to vapour between 290 and 350 °C.

The microthermometric data for the CH_4-dominant inclusions indicates the presence of additional volatiles. This is confirmed by laser Raman data. The inclusions with high Th_{CH_4} values contain higher hydrocarbons and those that show low Th_{CH_4} values or H0 behaviour contain H_2. The shift in peak positions away from published values at atmospheric pressure (Burke, 2001) for CH_4 (2917 cm^{-1}) and H_2 (4157 cm^{-1}) indicate that internal pressures in the inclusions may be as high as 400 bar (Seitz et al., 1993).

The fluid inclusion, laser Raman, and bulk gas data reported here clearly show that the peralkaline rocks of the Lovozero complex contain significant volumes of CH_4, H_2 and higher hydrocarbons. The gas chemistries of the fluid inclusions indicated by the microthermometric data and laser Raman analyses are similar to those obtained by bulk rock analysis. This could suggest that most of the gas within the rock is contained within the fluid inclusions. It also suggests that any gas held in sites other than fluid inclusions, such as along cleavage planes in nepheline or feldspar or in sealed microfractures, was trapped at the same time as that held in the inclusions.

5.1. PVTX modelling and fluid inclusion trapping conditions

Densities, and hence trapping pressures for the CH_4-dominant and H_2O-dominant inclusions were calculated using microthermometric and laser Raman data combined with data for the CH_4–C_2H_6 system (Olds, 1953) and H_2O–CH_4 system (Zhang and Frantz, 1992). Four types of CH_4-fluids were defined in the CH_4-dominant inclusion population; a high-density CH_4 fluid, a low-density CH_4 fluid, a low-density CH_4–H_2 mixed fluid (5–40 mol% H_2) and a low-density CH_4–C_2H_6 mixed fluid (1–40 mol% C_2H_6). It was not possible to constrain the compositional and volumetric properties of the H0 fluid inclusions containing CH_4 and H_2 due to lack of available published data on the CH_4–H_2 system and the unknown factors involved. The entrapment temperature for both the CH_4-dominant and H_2O-dominant inclusions was taken as 350 °C based on the evidence that these fluids were trapped at or near the CH_4–H_2O solvus in the two-phase field (see also Potter et al., 1998). Densities and entrapment pressures were therefore calculated for the fluid types at this temperature and their ranges shown in Table 4. The high-density CH_4 inclusions (Th-L) have an average density of ~ 0.25 g cm^{-3} and estimated entrapment pressures between 1.28 and 2.13 kbar, indicating formation depths between 4.2 and 7.0 km (assuming lithostatic pressures). These inclusions have been found to be most abundant in the borehole samples rather than in the near-surface hand specimens, consisting of ~ 40% of the inclusion population. From the tightly constrained range of Th_{CH_4}, predominantly between −80 and −85 °C, these high-density inclusions are assumed to be of a pure CH_4 composition. The low-density CH_4 inclusions (Th-V) have an average density of ~ 0.08 g cm^{-3} and entrapment pressures

Table 4
Calculated ranges of densities and pressures for fluid compositional types at 350 °C based on microthermometric and laser Raman data

FI type	Th_{CH_4} range (°C)		CH_4 range (mol%)	Density (ρ) range (g cm^{-3})	Pressure range (kbar)
High ρ CH_4	−82.0 to −99.0	L	100	0.24–0.31	1.28–2.13
Low ρ CH_4	−82.0 to −90.0	V	100	0.08–0.10	0.28–0.37
CH_4–HHC mix	−25.0 to −78.0	V	60–99	0.05–0.16	0.13–0.61
CH_4–H_2 mix	−88.0 to −120.0	V/Cr	60–90	0.02–0.07	0.09–0.29
H_2O-dom	[a]		–	–	0.50–1.00[a]

HHC: higher hydrocarbons.
[a] Pressures calculated from CH_4 clathrate melting temperatures (11–15.8 °C) based on Zhang and Frantz (1992).

between 0.28 and 0.37 kbar, indicating formation depths between 0.9 and 1.2 km. These inclusions are ubiquitous throughout all the samples but are most abundant in the near-surface hand specimens. The low-density CH_4–H_2 mixed fluid has an average density of $\sim 0.04\ g\ cm^{-3}$ and entrapment pressures between 0.09 and 0.29 kbar. This fluid type tends to be more commonly observed in the near-surface hand specimens. In contrast, the low-density CH_4–C_2H_6 mixed fluid tends to occur in the borehole samples. This fluid type has an average density of $\sim 0.06\ g\ cm^{-3}$ and entrapment pressures between 0.13 and 0.61 kbar. The H_2O-dominant inclusions estimated entrapment pressures were calculated from the observed CH_4 clathrate-melting temperatures and are between 0.5 and 1 kbar. It is evident that there is a broad pressure overlap for all fluid compositional types (0.1–1 kbar), with the exception of the high-density CH_4 population. The fluids are spatially heterogeneous with the high-density CH_4 population more commonly found in the deeper borehole samples. This fluid may represent a preserved, pure CH_4 fluid trapped at depth in the complex and overprinted by a later, low-density, more complex fluid. The low-density CH_4 fluids in the borehole samples tend to contain CH_4 and higher hydrocarbons whereas those found in the near-surface hand specimens contain CH_4 with abundant H_2. This may indicate that, at depth, higher hydrocarbons are more readily generated whereas, at shallower depths, CH_4 and H_2 are the dominant gas species. This spatial heterogeneity may explain the broad range of estimated trapping pressures calculated, with these fluids generated in localised environments at variable conditions.

6. Discussion

6.1. Models for the generation of abiogenic hydrocarbons in Lovozero and other igneous complexes

In a review of the relevant literature, Potter and Konnerup-Madsen (2003) showed that there are two likely models for the generation of abiogenic hydrocarbons in igneous rocks. These are the late-magmatic model (e.g., Karzhavin and Vendillo, 1970; Gerlach, 1980; Konnerup-Madsen et al., 1981; Kogarko et al., 1987) and the postmagmatic model (e.g., Abrajano et al., 1990; Sherwood-Lollar et al., 1993; Salvi and Williams-Jones, 1997; Potter et al., 1998). The key points of these two models are laid out below.

6.1.1. The late-magmatic model

Konnerup-Madsen et al. (1981, 1985) and Konnerup-Madsen (1988) showed that it is possible to evolve a CH_4-rich fluid by respeciation of a carbonic fluid in the C–O–H–graphite system under magmatic conditions at geologically feasible fO_2 conditions (i.e., QFM to QFM-3) below 500 °C. This process has been advocated for CH_4 generation in metamorphic rocks (Holloway, 1984; Cesare, 1995) but can only occur in igneous rocks at unusually low solidus temperatures. Such temperatures can be achieved in volatile-rich agpaitic magmas where the solidus may be depressed as low as 450 °C (e.g., Sørensen, 1997). This model could therefore explain the presence of hydrocarbons in the agpaitic rocks of the Lovozero complex, as well as the associated Khibina complex and Ilímaussaq complex in Greenland. However, it cannot be applied to igneous terranes where the magmas have higher solidus temperatures (i.e., miaskitic alkaline and ultrabasic rocks), and it does not satisfactorily explain the lack of graphite reported in rocks from Lovozero, or the generation of significant amounts of H_2 and higher hydrocarbons present in the fluids at Lovozero and other peralkaline complexes.

6.1.2. The postmagmatic model

A number of authors have suggested that abiogenic hydrocarbons could be generated in a variety of igneous rocks by postmagmatic Fischer–Tropsch (F–T) type reactions (e.g., Szatmari, 1989; Abrajano et al., 1990; Sherwood-Lollar et al., 1993; Sugisaki and Mimura, 1994; Kelley, 1996; Salvi and Williams-Jones, 1997; Potter et al., 1998). The production of hydrocarbons by F–T synthesis is well documented in the chemical industry, where F–T reactions convert combusted coal to petroleum through a series of disequilibrium reactions that can be represented by:

$$n\mathrm{CO} + (2n+1)\mathrm{H_2} \rightarrow \mathrm{C}_n\mathrm{H}_{2n+2} + n\mathrm{H_2O} \quad \text{(R1)}$$

$$n\mathrm{CO_2} + (3n+1)\mathrm{H_2} \rightarrow \mathrm{C}_n\mathrm{H}_{2n+2} + 2n\mathrm{H_2O} \quad \text{(R2)}$$

At temperatures below 400 °C at 0.1 kbar, long chains of hydrocarbons can be produced. However, higher hydrocarbons, up to C_6, can still form at temperatures of 600 °C at these low pressures (Anderson, 1984). In industry, the F–T reaction is catalysed

by the presence of group VIII metals and oxides, specifically Fe (Anderson, 1984), and it has been reported that Fe-silicates and hydrated silicates (zeolites) can also act as catalysts (Lancet and Anders, 1970; Porfir'ev, 1974; Szatmari, 1989).

F–T synthesis can be applied to hydrocarbon generation under natural conditions. Such a synthesis requires postmagmatic mineral–fluid reactions that involve a suitable mineral assemblage, a primary CO_2-rich fluid and a source of H_2. CH_4 production in ultrabasic rocks during serpentinization has been attributed to the operation of F–T reactions (Porfir'ev, 1974; Szatmari, 1989; Abrajano et al., 1990; Sherwood-Lollar et al., 1993; Sugisaki and Mimura, 1994; Kelley, 1996; Berndt et al., 1996). In such cases, the H_2 required to drive F–T synthesis can be generated during serpentinization by reactions involving oxidation of Fe^{2+} to Fe^{3+} and release of H_2 (i.e., olivine to serpentine and magnetite).

Similar reactions can occur in alkaline igneous rocks. Salvi and Williams-Jones (1997) suggested that hydrocarbons present in the Strange Lake peralkaline granitic complex in Canada were generated by F–T reactions during late-stage hydrothermal alteration of Fe-rich minerals, such as arfvedsonite resulting in the production of H_2 by the reaction:

$$\underset{\text{Arfvedsonite}}{3Na_3Fe_4^{2+}Fe^{3+}Si_8O_{22}(OH)_2} + 2H_2O \rightarrow \underset{\text{Aegirine}}{9NaFe^{3+}Si_2O_6} + \underset{\text{Magnetite}}{2Fe_3O_4} + \underset{\text{Quartz}}{6SiO_2} + 5H_2 \quad (R3)$$

Potter et al. (1998) further suggested that an F–T process could explain CH_4 production in the Khibina complex. In that case, H_2 was thought to have been produced through postmagmatic hydrothermal reactions, which involved the alteration of the primary mineral assemblage of nepheline, augite and Ti-magnetite to magnetite, biotite, aegirine and zeolites. For example:

$$\underset{\text{Augite}}{4(CaNa)(Fe^{2+})Si_2O_6} + \underset{\text{Ti-Magnetite}}{3(Fe_2^{2+}Ti)O_4} + \underset{\text{Nepheline}}{NaAlSiO_4} + \underset{\text{Kalsilite}}{2KAlSiO_4} + 2Si^{4+} + 8H_2O \rightarrow \underset{\text{Biotite}}{K_2Fe_6^{2+}(AlTi)_2Si_6O_{20}(OH)_4} + \underset{\text{Magnetite}}{Fe_2^{3+}Fe^{2+}O_4} + \underset{\text{Aegirine}}{NaFe^{3+}Si_2O_6} + \underset{\text{Titanite}}{2CaTiSiO_5} + \underset{\text{Natrolite}}{Na2Al_2Si_3O_{10}\cdot 2H_2O} + 2H_2O + 3H_2 \quad (R4)$$

Therefore, the F–T model can be applied to a variety of igneous terranes and can potentially explain the gas assemblages identified including the production of higher hydrocarbons and H_2. Evidence for this model is discussed in the next section in the context of the new Lovozero data reported here as well as other data from Lovozero and similar complexes published elsewhere.

6.2. Evidence for the origin of hydrocarbon-bearing fluids in Lovozero and related plutons

6.2.1. Fluid inclusion evidence

It is apparent from the reported fluid inclusion data in the Lovozero complex that the CH_4-dominant (and H_2O-dominant) inclusions were trapped during postmagmatic alteration processes along fractures and cleavage planes (Fig. 2). This is supported by the estimated entrapment temperatures (ca. 350 °C). Textural evidence from the Lovozero complex reveals a close spatial relationship between CH_4-dominant inclusions and Fe-rich minerals, in this case, arfvedsonite and aegirine, as well as the zeolites, analcite and natrolite (Fig. 2). This association is similar to that described at Khibina (Potter et al., 1998). However, the dominant relationship preserved in the less alkaline miaskitic rocks of the Khibina complex, such as the apatite–nepheline ores, is between CH_4-dominant inclusions and titanomagnetite, aegirine, biotite, magnetite and natrolite (Potter et al., 1998). In the more alkaline agpaitic rocks of both the Khibina and Lovozero complexes, aegirine rather than magnetite is the stable Fe phase (Korobeynikov, 1994), and is also spatially associated with the CH_4-dominant inclusions (Fig. 2). These spatial signatures are similar to those reported from Ilímaussaq where hydrocarbon-bearing inclusions are associated with aegirine (Konnerup-Madsen et al., 1985) and in the Strange Lake granite where they are associated with arfvedsonite, aegirine and magnetite (Salvi and Williams-Jones, 1997). Significantly, in both the Lovozero and Strange Lake complexes, abundant H_2 (up to 40 mol%) is present in inclusions associated with the replacement of arfvedsonite by aegirine. In the Strange Lake complex, the H_2 can be generated by the operation of reaction (3). In the absence of

magnetite, H_2 in the Lovozero complex was probably produced by the reaction:

$$\underset{\text{Arfvedsonite}}{Na_3\,Fe_4^{2+}Fe^{3+}Si_8O_{22}(OH)_2} + 2\underset{\text{Nepheline}}{NaAlSiO_4} + 4H_2O \rightarrow 5\underset{\text{Aegirine}}{NaFe^{3+}Si_2O_6} + 2Al(OH)_3^0 + 2H_2 \quad (R5)$$

for which there is good textural evidence (Fig. 2).

The textural observations described are consistent with the hypothesis that the hydrocarbons were generated in F–T type reactions during postmagmatic alteration of the mineral assemblages, involving reactions between a CO_2-rich fluid and H_2 generated during alteration reactions, that specifically affected Fe-rich minerals. The close spatial association between the CH_4-dominant inclusions and the Fe-rich minerals suggest that the latter phases play an important role in catalysing F–T reactions. The spatial heterogeneity of the composition of the CH_4-dominant inclusions throughout the Lovozero complex would also indicate that the fluids were generated during postmagmatic processes, controlled by local environmental factors (e.g., pressure, temperature, geochemistry). This would seem to contradict the late-magmatic model with formation of a CH_4-rich fluid, in equilibrium with, and buffered by a subsolidus agpaitic magma. Although, in this study, little evidence has been found for an early CO_2-rich fluid at Lovozero; a CO_2-rich magmatic fluid in the associated alkaline intrusion at Khibina has been identified in the sulphide-rich carbonatite (Potter, 2000). This fluid may represent the early magmatic CO_2-rich fluid generated in such complexes that has only been preserved in the Khibina carbonatite due to the nature

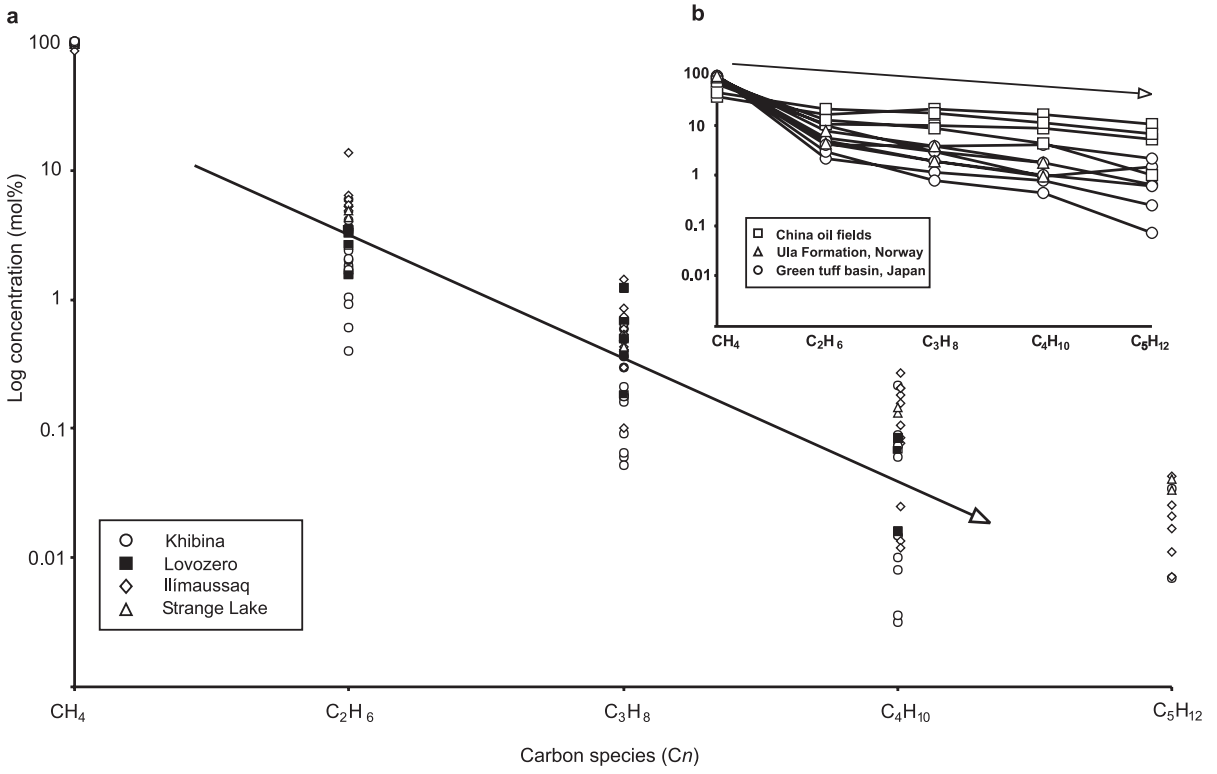

Fig. 6. (a) A plot of log normalised abundances of hydrocarbon species (mol%) for the abiogenic hydrocarbon-bearing fluids at Khibina, Lovozero, Ilímaussaq and Strange Lake. (b) For comparison, the distribution of hydrocarbon species in biogenically derived hydrocarbon gases are shown for the China oil fields (average mol%), the Ula Formation, Norway and thermogenic gases in the Green Tuff Basin, Japan. Arrows represent general slope in distribution of hydrocarbon species. (Data from Petersilie et al., 1961; Petersilie, 1962; Petersilie and Sørensen, 1970; Konnerup-Madsen et al., 1979; Konnerup-Madsen and Rose-Hansen, 1982; Voytov, 1992; Karlsen et al., 1993; Sakata et al., 1997; Salvi and Williams-Jones, 1997; Chen et al., 2000.)

of the rock type. This may imply that, in similar circumstances, possibly at depth in the Lovozero complex, a similar early CO_2-rich fluid may be preserved.

6.2.2. Bulk gas evidence

The mass spectrometer data from the Lovozero samples show significant concentrations of higher hydrocarbons up to C_5 and C_6 (Fig. 5). Relative concentrations decrease with increasing carbon number (Cn). As quantitative concentrations were not obtained with this technique and the gas-chromatographic method was also limited in detection, quantitative gas data from the literature for Lovozero and the other hydrocarbon-bearing igneous complexes, Khibina, Ilímaussaq and Strange Lake, are combined and discussed in regard to the two models (see review by Potter and Konnerup-Madsen, 2003). A plot of the distribution of hydrocarbon species according to carbon number in these fluids can be produced from these data and is shown in Fig. 6a. This normalised log diagram shows that the hydrocarbons have a typical Schulz–Flory distribution with a log-linear decrease in concentration with increasing Cn (Anderson, 1984). Although this linear distribution is indicative of many pathways for formation of hydrocarbons (Kissin, 1987), the steep slope observed for these hydrocarbon-bearing fluids, as indicated by the arrow, is very different to those seen for biogenically derived hydrocarbons (Fig. 6b). The C*n* ratios calculated from the bulk gas data are low for all the complexes (Table 5). Those for C_2/C_1 are between 0.01 and 0.12, indicating a predominance of CH_4. The ratio between the higher hydrocarbon species increases and levels out at an average of ~ 0.3. The C*n* ratios, as well as the steep sloped log-linear distribution is well known in industry for hydrocarbons generated by F–T synthesis, with a constant Cn ratio that does not exceed 0.6 (Anderson, 1984). Thus, the bulk gas concentration data for the hydrocarbon-bearing fluids from Lovozero and Khibina, as well as other alkaline complexes, are consistent with derivation through abiogenic F–T reactions, supporting the postmagmatic model.

6.2.3. Isotopic evidence

Detailed isotopic studies have been carried out on the fluids in Lovozero and Khibina by Nivin et al. (1988, 1993, 1995) and Voytov (1992). The $\delta^{13}C$ and δD isotopic data for these fluids are listed in Table 6. For gases released from fluid inclusions during crushing and for free gases extracted from boreholes, the $\delta^{13}C$ values for CH_4 range from $-3‰$ to $-16‰$. These data indicate either a heterogeneous source or process for hydrocarbon generation. δD_{CH_4} values have a range of $-132‰$ to $-167‰$. The $\delta^{13}C$ values between $-3‰$ and $-16‰$ would tend to exclude a biogenic origin, falling outside any defined biogenic fields, and therefore favour an abiogenic origin (Schoell, 1988). The $\delta^{13}C$ values recorded for the higher hydrocarbons are also indicative of an abiogenic origin (Table 6). These show a decrease in $\delta^{13}C$ values with increasing carbon number. This implies that successive formation of higher hydrocarbons, possibly through polymerisation of

Table 5
Carbon number ratios calculated from published bulk gas data from Potter and Konnerup-Madsen (2003)

Rock type	C_2/C_1	C_3/C_2	C_4/C_3	C_5/C_4
Lovozero				
Juvite	0.07	0.08	0.59	–
Syenite	0.05	0.21	0.06	–
Foyaite	0.03	0.47	0.19	–
Khibina				
Nepheline syenite	0.01	0.22	0.21	–
Rischorrite	0.08	0.24	0.41	–
Ijolite	0.04	0.26	0.27	0.55
Kukisvumchorr mine	0.07	0.25	0.18	0.28
Rasvumchorr mine	0.05	0.13	0.24	0.18
Rasvumchorr mine	0.07	0.08	0.10	–
Khibinite	0.03	0.05	0.01	–
Rischorrite	0.04	0.05	0.05	–
Ilímaussaq				
Syenite	0.03	0.09	0.18	–
Naujaite	0.12	0.18	0.28	–
Foyaite	0.10	0.18	0.28	–
Lujavrite	0.13	0.07	0.05	–
Sodalite + nepheline	0.12	0.15	0.31	0.13
Arfvedsonite	0.09	0.13	0.38	0.03
Sodalite	0.12	0.21	0.32	–
Sodalite	0.10	0.15	0.25	0.25
Arfvedsonite	0.10	0.13	0.24	0.11
Nepheline	0.11	0.13	0.24	0.12
Eudialyte	0.30	0.15	0.25	0.12
Strange lake				
Fresh pegmatite	0.08	0.18	0.34	0.34
Altered pegmatite	0.10	0.14	0.41	0.34

Table 6
Compiled published carbon and deuterium isotopic ratios for fluids in Lovozero and Khibina

Sample	δD_{H_2} (‰)	δD_{CH_4} (‰)	$\delta^{13}C_{CH_4}$ (‰)	$\delta^{13}C_{C_2H_6}$ (‰)	$\delta^{13}C_{C_3H_8}$ (‰)	$\delta^{13}C_{CO_2}$ (‰)
Lovozero						
Urtite[a]	−629.0	−164.0	–	–	–	–
Foyaite[a]	−198.0	n.d.	–	–	–	–
Foyaite[a]	−448.0	−132.0	–	–	–	–
Urtite[a]	−359.0	n.d.	–	–	–	–
Urtite[a]	−644.0	−167.0	–	–	–	–
Urtite[a]	−609.0	n.d.	–	–	–	–
Foyaite[a]	−604.0	n.d.	−11.8	−15.2	–	–
Foyaite[a]	n.d.	−167.0	–	–	–	–
Free gas[b]			−7.1 to −15.7			
Khibina						
Carbonatite[c]	–	–	–	–	–	−7.3
Urtite[d]	–	–	−12.8	−24.0	−26.0	–
Khibinite[d]	–	–	−3.2	−9.1	−25.7	–
Eudialyte[d]	–	–	−7.9	−14.2	n.d.	–
Free gas[e]	–	–	−10.6	n.d.	−23.9	–
Free gas[e]	–	–	−6.5	−11.7	n.d.	–
Rasvumchorr mine[e]	–	–	−11.2	−15.6	n.d.	–
Free gas[b]	–	–	−7.7 to −14.0	n.d.	n.d.	–

n.d.: Not detected.
[a] Nivin et al. (1995).
[b] Nivin et al. (2001).
[c] Potter (2000).
[d] Voytov (1992) in inclusions.
[e] Voytov (1992) in free gases.

methyl radicals by F–T type reactions, occurred rather than cracking of complex organic matter, which would give an inverse relationship between $\delta^{13}C$ and C*n* (Des Marais et al., 1981; Sherwood-Lollar et al., 2002). This can be demonstrated in Fig. 7 where published $\delta^{13}C_{Cn}$ data for the hydrocarbon-bearing fluids at Khibina and Lovozero are plotted alongside data from thermogenic (biogenic) hydrocarbons from oil fields and geothermal springs.

Helium and argon isotope data for fluids from Lovozero are reported by Nivin et al. (1988, 1993). The $^3He/^4He$ ratios are between 1×10^{-8} and 25×10^{-8} and $CH_4/^3He$ ratios between 3×10^9 and 15×10^9. The $^{40}Ar/^{36}Ar$ ratios are variable, ranging from 600 to 8000. Based upon values calculated from evolutionary models for terrestrial gas reservoirs for He, Ar and CH_4, contributions of mantle, crust and atmospheric input can be estimated (Prasolov and Tolstikhin, 1987; Tolstikhin and Marty, 1998). The $^3He/^4He$ ratios indicate a predominantly radiogenic, crustal input for the fluids with a maximimum of 2% He mantle input. The $CH_4/^3He$ ratios indicate a maximum of 10% mantle CH_4 input. The wide range in $^{40}Ar/^{36}Ar$ ratios indicates variable contamination from crustal and atmospheric sources. On average, these values are consistent with mantle, crustal and atmospheric inputs of 2%, 98% and <0.1%, respectively, for the analysed fluids (Nivin et al., 1993).

Nivin et al. (1995) also showed, on the basis of equilibrium calculations on the isotopic pairs for $\delta D_{CH_4}-\delta D_{H_2O}$ and $\delta D_{H_2}-\delta D_{H_2O}$ using the δD_{CH_4} and δD_{H_2} values shown in Table 6, that the hydrocarbon-bearing fluids at Lovozero could not have been in equilibrium with each other, giving highly variable estimated formation temperatures between the isotopic pairs. The δD_{H_2} signatures (~ -600‰) are consistent with H_2 generation through low-temperature processes (Bottinga, 1969; Devirts et al., 1993). For example, the δD_{H_2} values

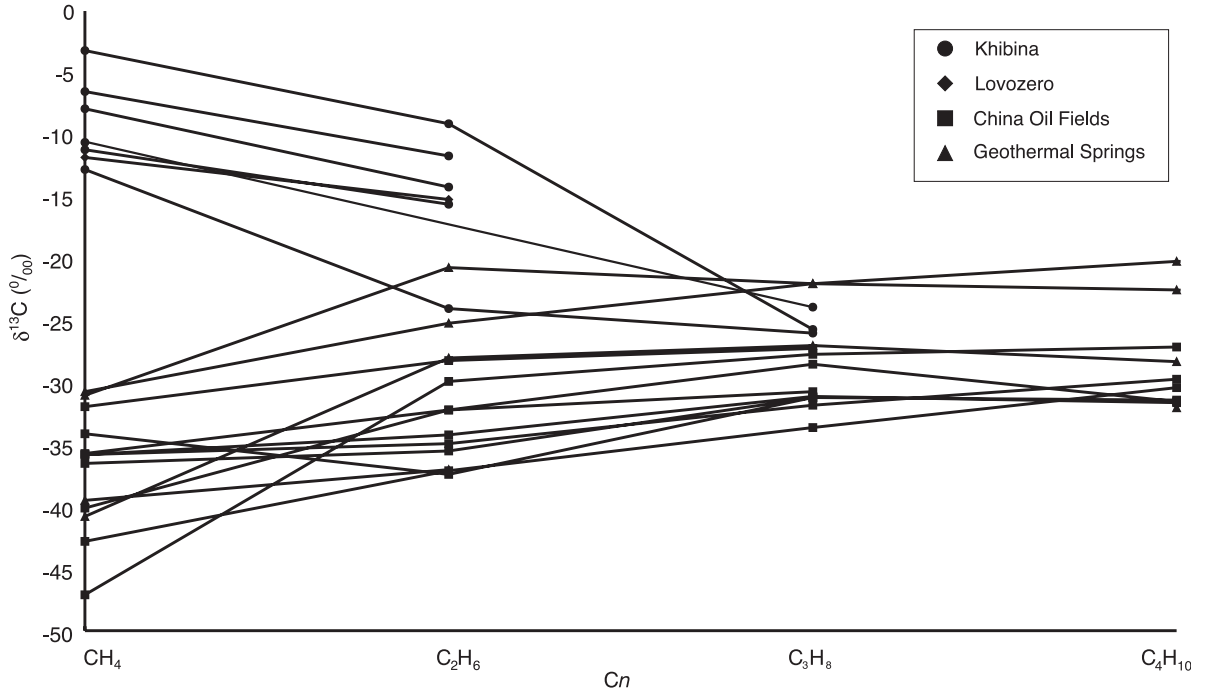

Fig. 7. A plot showing the distribution of $\delta^{13}C$ values with increasing carbon number (Cn) for the abiogenic hydrocarbon gases at Khibina (Voytov, 1992) and Lovozero (Nivin et al., 1993), and for comparison, biogenic gases from the China oil fields (Dai et al., 1996; Chen et al., 2000) and various geothermal springs, USA (Des Marais et al., 1981). Taken from Potter and Konnerup-Madsen (2003).

are similar to those for H_2 generated in serpentinized ultrabasic rocks (Neal and Stanger, 1983; Abrajano et al., 1990; Sherwood-Lollar et al., 1993). Therefore, these combined data support a model of fluid formation during a postmagmatic crustal process (i.e., hydrothermal alteration during interactions with crustal H_2O) that involved disequilibrium reactions such as F–T reactions. They are not consistent with the late-magmatic model. The large variation in $\delta^{13}C_{CH_4}$ values (-3‰ to -16‰) would also support this model. The CH_4 formed from a primary magmatic CO_2-rich fluid at early stages would have a lighter signature than CH_4 formed at later stages, which would approach the initial mantle carbon signature of the primary magmatic CO_2-rich fluid as it was consumed (Lancet and Anders, 1970; Voytov, 1992). This early magmatic CO_2-rich fluid could be represented by the CO_2-rich fluid identified in the Khibina carbonatite with a $\delta^{13}C_{CO_2}$ value of -7‰ (Table 4), clearly in the mantle field.

6.3. Summary and wider implications for the F–T model

From the data presented and discussed above, it can be concluded that although the late-magmatic model could still be viable for generation of hydrocarbons in the Ilímaussaq complex as presented by Konnerup-Madsen et al. (1985) and hence for other agpaitic rocks, it is not favoured here. The fluid inclusion, compositional, bulk gas and isotopic data on the hydrocarbon-bearing fluids in the Lovozero and Khibina complexes, along with the textural evidence would strongly suggest that the hydrocarbons were generated postmagmatically by F–T synthesis. The relationship between the hydrocarbon-bearing fluid inclusions and Fe phases and zeolitization is apparent in all igneous rock types. The less alkaline miaskitic rocks in complexes (e.g., Khibina and Strange Lake) show close associations between the inclusions and magnetite, biotite and arfvedsonite. The more alkaline agpaitic rocks in

complexes, e.g., Lovozero and Ilímaussaq, show close associations between the inclusions and aegirine and arfvedsonite. These relationships provide a key to understanding how, and in what environments hydrocarbon-generating reactions can occur. The presence of Fe-rich phases and the incipient alteration of these phases may not only generate the H_2 required for F–T reactions but may also act as the surface catalysts for F–T synthesis. Therefore, the main controlling factor for the formation of abiogenic hydrocarbons in igneous rocks may be the total Fe content of the igneous assemblage. A further example of this is the widespread report of abiogenic hydrocarbons found in association with ultrabasic igneous rocks, formed during the alteration of olivine to serpentine and magnetite. However, another potential controlling factor may be the bulk chemistry of the igneous assemblage. Calculations by Ryzhenko and Kraynov (1992), investigating H_2 formation in hydrothermal waters during interaction with Fe–Al silicates, found that H_2 production reached a maximum in alkaline fluids in contact with alkaline and ultrabasic igneous rocks. Therefore, a relationship between Fe and Na + K/Si contents of the igneous rocks may be the combined controlling factor for predicting where abiogenic hydrocarbons are generated and in what igneous complexes.

A limitation on the production of abiogenic hydrocarbons could be that in order to generate and trap these hydrocarbons within the igneous rock assemblages, incipient hydration of a primary mineral assemblage is required. Preliminary fluid inclusion work on the alkaline Sokli carbonatite complex, which contains many Fe-rich phases (Potter, 2000) in Finland showed the presence of only very small concentrations of hydrocarbons in discrete areas. In contrast to Lovozero and Khibina, Sokli is characterised by large-scale alteration including serpentinization and phlogopitization. It would appear in this case that pervasive alteration swamped the system with H_2O and flushed out any hydrocarbons that may have formed. At Sokli, the presence of abundant sulphides may also be a factor for the lack of hydrocarbons, as the presence of sulphur is known to poison the catalysts used in F–T synthesis (Madon and Taylor, 1981). This may explain the preservation of the CO_2-rich fluid in the sulphide-rich carbonatite at Khibina. Another limitation may be the rate at which the F–T reactions can take place. Recent laboratory experiments on CH_4 production through F–T reactions during serpentinization have indicated that CH_4 production is slow and that the F–T reaction may not be as effective in natural mineral assemblages as previously proposed (Berndt et al., 1996; Horita and Berndt, 1999; McCollom and Seewald, 2001).

Acknowledgements

We thank Valentin Nivin for providing GC gas data and Don Hall (FIT) for quadrupole analysis of samples from Lovozero. Discussions with Alan Woolley, John Clemens, Chris Clayton, Valentin Nivin and Jens Konnerup-Madsen and comments and reviews on earlier versions of this manuscript from Stef Salvi, Bob Burruss, Tom Andersen and Martin Feely are gratefully acknowledged. This project was funded by the European Union (INTAS award 1010-CT 93-0007) and Kingston University.

References

Abrajano, T.A., Sturchio, N.C., Kennedy, B.M., Lyon, G.L., Muehlenbachs, K., Bohlke, J.K., 1990. Geochemistry of reduced gas related to serpentinization of the Zambales ophiolite, Philippines. Appl. Geochem. 5, 625–630.

Anderson, R.B., 1984. The Fischer–Tropsch Synthesis. Academic Press, New York, USA.

Bakker, R.J., 2001. FLUIDS: a new software package to handle microthermometric data and to calculate isochores. ECROFI XVI. Faculdade de Ciencias do Porto, Departmento de Geologia, Memoria 7, Porto, pp. 23–25.

Berndt, M.E., Allen, D.E., Seyfried, W.E., 1996. Reduction of CO_2 during serpentinization of olivine at 300 °C and 500 b. Geology 24, 351–354.

Bottinga, Y., 1969. Calculated fractionation factors for carbon and hydrogen isotope exchange in the system calcite–carbon dioxide–methane–hydrogen–water vapour. Geochim. Cosmochim. Acta 33, 49–64.

Brown, P.E., Lamb, W.M., 1989. $P–V–T$ properties of fluids in the system $H_2O \pm CO_2 \pm NaCl$: new graphical representations and implications for fluid inclusion studies. Geochim. Cosmochim. Acta 53, 1209–1221.

Burke, E.A.J., 2001. Raman microspectrometry of fluid inclusions. Lithos 55, 139–158.

Cesare, B., 1995. Graphite precipitation in C–O–H fluid inclusions: closed system compositional and density changes and thermobarometric implications. Contrib. Mineral. Petrol. 122, 25–33.

Chen, J., Xu, Y., Huang, D., 2000. Geochemical characteristics and origin of natural gas in Tarim Basin, China. AAPG Bull. 84 (5), 591–606.

Dai, J., Song, Y., Dai, C., Wang, D., 1996. Geochemistry and accumulation of carbon dioxide gases in China. AAPG Bull. 80 (10), 1615–1626.

Des Marais, D.J., Donchin, J.H., Nehring, N.L., Truesdell, A.H., 1981. Molecular carbon isotopic evidence for the origin of geothermal hydrocarbons. Nature 292, 826–828.

Devirts, A.L., Gagauz, F.G., Grinenko, V.A., Lagutina, Ye.P., Pereverzov, V.V., Shukolyukov, Yu.A., 1993. Origin of hydrogen in Kempirsay-intrusion ultramafites. Geochem. Int. 30 (2), 139–144.

Duan, Z., Møller, N., Weare, J.H., 1992. Molecular dynamics simulation of *PVT* properties of geological fluids and a general equation of state of nonpolar and weakly polar gases up to 2000 K and 20,000 bar. Geochim. Cosmochim. Acta 56, 3839–3845.

Duan, Z., Møller, N., Weare, J.H., 1995. An equation of state for the $NaCl–CO_2–H_2O$ system: prediction of phase equilibria and volumetric properties. Geochim. Cosmochim. Acta 59, 2869–2882.

Duan, Z., Møller, N., Weare, J.H., 1996. A general equation of state for supercritical fluid mixtures and molecular dynamics simulation of mixture PVTX properties. Geochim. Cosmochim. Acta 60, 1209–1216.

Dudkin, O.B., Mitrofanov, F.P., 1994. Features of the Kola Alkali Province. Geochem. Int. 31 (3), 1–11.

Fluid Inclusion Technologies website. http://www.fittulsa.com.

Gerasimovsky, V.K., Volkov, V.P., Kogarko, L.N., Polyakov, A.I., Saprynka, T.V., Balashov, Yu.A., 1968. The Geochemistry of the Lovozero Alkaline Massif. Australian National Univ. Press, Canberra, Australia.

Gerlach, T.M., 1980. Chemical characteristics of the volcanic gases from Nyiragongo Lava Lake and the generation of CH_4-rich fluid inclusions. J. Volcanol. Geotherm. Res. 8, 177–189.

Gold, T., 1979. Terrestrial sources of carbon and earthquake outgassing. J. Pet. Geol. 1 (3), 3–19.

Holloway, J.R., 1984. Graphite–CH_4–H_2O–CO_2 equilibria at low grade metamorphic conditions. Geology 12, 455–458.

Horita, J., Berndt, M.E., 1999. Abiogenic methane formation and isotopic fractionation under hydrothermal conditions. Science 285, 1055–1057.

Ikorski, S.V., Voloshin, A.V., 1982. Typical gas-phase compositions in inclusions in quartz from Kola Peninsula granite pegmatites. I. Geochem. Int. 19 (5), 173–179.

Ikorski, S.V., Nivin, V.A., Pripachkin, V.A., 1992. Gas Geochemistry of Endogenic Formations. Nauka, St. Petersburg, Russia. In Russian.

Karlsen, D.A., Nedkvitne, T., Larter, S.R., Bjørlykee, K., 1993. Hydrocarbon composition of authigenic inclusions: application to elucidation of petroleum reservoir filling history. Geochim. Cosmochim. Acta 57, 3641–3659.

Karzhavin, V.K., Vendillo, V.P., 1970. Thermodynamic equilibrium and conditions for existence of hydrocarbon gases in a magmatic process. Geochem. Int. 7, 797–803.

Kelley, D.S., 1996. Methane rich fluids in the oceanic crust. J. Geophys. Res. 101 (B2), 2943–2962.

Kissin, Y.V., 1987. Catagenesis and composition of petroleum: origin of *n*-alkanes and isoalkanes in petroleum crudes. Geochim. Cosmochim. Acta 51, 2445–2457.

Kogarko, L.N., Kosztolanyi, Ch., Ryabchikov, I.D., 1987. Geochemistry of the reduced fluid in alkali magmas. Geochem. Int. 24 (7), 20–27.

Kogarko, L.N., Kononova, V.A., Orlova, M.P., Woolley, A.R., 1995. Alkaline Rocks and Carbonatites of the World: Part 2. Former USSR. Chapman & Hall, London, UK.

Konnerup-Madsen, J., 1988. Abiogenic hydrocarbon gases. In: Santosh, M. (Ed.), Fluid Inclusions. Spec. Mem. Geol. Soc. India, pp. 13–24.

Konnerup-Madsen, J., Rose-Hansen, J., 1982. Volatiles associated with alkaline igneous activity: fluid inclusions in the Ilímaussaq intrusion and the Gardar granitic complexes (South Greenland). Chem. Geol. 37, 79–93.

Konnerup-Madsen, J., Larsen, E., Rose-Hansen, J., 1979. Hydrocarbon-rich fluid inclusions in minerals from the alkaline Ilímaussaq intrusion, South Greenland. Bull. Soc. Fr. Mineral. Cristallogr. 102, 642–653.

Konnerup-Madsen, J., Rose-Hansen, J., Larsen, E., 1981. Hydrocarbon gases associated with alkaline igneous activity: evidence from composition of fluid inclusions. Rapp.-Grønl. Geol. Unders. 103, 99–108.

Konnerup-Madsen, J., Dubessy, J., Rose-Hansen, J., 1985. Combined Raman microprobe spectrometry and microthermometry of fluid inclusions in minerals from igneous rocks of the Gardar Province (South Greenland). Lithos 18, 271–280.

Korobeynikov, A.A., 1994. Petrological aspects of the evolution of clinopyroxene compositions in the intrusive rocks of the Lovozero alkaline massif. Geochem. Int. 31 (3), 69–76.

Kramm, K., Kogarko, L.N., Kononova, V.A., Vartianen, H., 1993. The Kola Alkaline Province of the CIS and Finland: precise Rb–Sr ages define 380–360 Ma age range for all magmatism. Lithos 30, 33–44.

Kretz, R., 1983. Symbols for rock-forming minerals. Am. Mineral. 68, 277–279.

Lancet, M.S., Anders, E., 1970. Carbon isotope fractionation in the Fischer–Tropsch synthesis and in meteorites. Science 170, 981–983.

Madon, R.J., Taylor, W.F., 1981. Fischer–Tropsch synthesis on precipitated Fe catalyst. J. Catal. 69, 32–43.

McCollom, T.M., Seewald, J.S., 2001. A reassessment of the potential for reduction of dissolved CO_2 to hydrocarbons during serpentinization of olivine. Geochim. Cosmochim. Acta 65 (21), 3679–3778.

Neal, C., Stanger, G., 1983. Hydrogen generation from mantle source rocks in Oman. Earth Planet. Sci. Lett. 60, 315–321.

Nivin, V.A., Kamenskiy, I.L., Tolstikhin, I.N., 1988. Helium and argon isotope compositions in rocks of the ore horizons of the Lovozero massif. Geochem. Int. 25 (8), 27–32.

Nivin, V.A., Kamenskiy, I.L., Tolstikhin, I.N., 1993. Helium and argon isotope abundances in rocks of Lovozero alkaline massif. Isotopenpraxis 28, 281–287.

Nivin, V.A., Devirts, A.L., Lagutina, Ye.P., 1995. The origin of the gas phase in the Lovozero massif based on hydrogen-isotope data. Geochem. Int. 32 (8), 65–71.

Nivin, V.A., Belov, N.I., Treloar, P.J., Timofeyev, V.V., 2001. Relationships between gas geochemistry and release rates and the stressed state of igneous rock massifs. Tectonophysics 336 (1–4), 233–244.

Olds, R.H., 1953. Critical behaviour of hydrocarbons. In: Farkas, A. (Ed.), Physical Chemistry of the Hydrocarbons. Academic Press, New York, USA, pp. 131–152.

Petersilie, I.A., 1962. Origin of hydrocarbon gases and dispersed bitumens of the Khibina alkalic massif. Geochem. Int. 1, 14–29.

Petersilie, I.A., Sørensen, H., 1970. Hydrocarbon gases and bituminous substances in rocks from the Ilímaussaq alkaline intrusion, South Greenland. Lithos 3, 59–76.

Petersilie, I.A., Ikorski, S.V., Smirnova, L.I., Romanikhin, A.M., Proskuryakova, E.B., 1961. Application of gas logging to the investigation of natural gases and bitumens in the Khibina intrusive massif. Geochem. Int. 10, 945–962.

Porfir'ev, V.B., 1974. Inorganic origin of petroleum. AAPG Bull. 58 (1), 3–33.

Potter, J., 2000. The characterisation and origin of hydrocarbons in alkaline igneous rocks of the Kola Alkaline Province. PhD Thesis. Kingston University, London, UK.

Potter, J., Konnerup-Madsen, J., 2003. A review of the occurrence and origin of abiogenic hydrocarbons in igneous rocks. In: Petford, N., McCaffrey, K.J.W. (Eds.), Hydrocarbons in Crystalline Rocks. Spec. Publ.-Geol. Soc., London, vol. 214, pp. 151–173.

Potter, J., Rankin, A.H., Treloar, P.J., Nivin, V.A., Ting, W., Ni, P., 1998. A preliminary study of methane inclusions in alkaline igneous rocks of the Kola Igneous Province, Russia: implications for the origin of methane in igneous rocks. Eur. J. Mineral. 10, 1167–1180.

Prasolov, E.M., Tolstikhin, I.N., 1987. Juvenile gases He, CO_2, CH_4—their relations and contributions to the fluids of earth's crust. Geokhimiya 10, 1406–1414 (in Russian).

Roedder, E., 1984. Fluid Inclusions, vol. 12. Mineralogical Society of America, USA.

Ryzhenko, B.N., Kraynov, S.R., 1992. Causes of hydrogen accumulation and reduction in hydrothermal fluids. Geochem. Int. 29 (12), 1–8.

Sakata, S., Sano, Y., Maekawa, T., Igari, S.I., 1997. Hydrogen and carbon isotopic composition of methane as evidence for biogenic origin of natural gases from the Green Tuff Basin, Japan. Org. Geochem. 26 (5/6), 399–407.

Salvi, S., Williams-Jones, A.E., 1997. Fischer–Tropsch synthesis of hydrocarbons during sub-solidus alteration of the Strange Lake peralkaline granite, Quebec/Labrador, Canada. Geochim. Cosmochim. Acta 61 (1), 83–99.

Salvi, S., Williams-Jones, A.E., 2003. Bulk analysis of volatiles in fluid inclusions. In: Samson, I.M., Anderson, A., Marshall, D. (Eds.), Fluid Inclusions: Analysis and Interpretation. Short Course. Mineral. Soc. Can. vol. 32, pp. 247–278.

Schoell, M., 1988. Multiple origins of methane in the earth. Chem. Geol. 71 (1–3), 1–10.

Seitz, J.C., Pasteris, J.D., Chou, I., 1993. Raman spectroscopic characterization of gas mixtures: I. Quantitative composition and pressure determination of CH_4–N_2 and their mixtures. Am. J. Sci. 293, 297–321.

Shepherd, T.J., Rankin, A.H., Alderton, D.H.M., 1985. A Practical Guide to Fluid Inclusion Studies. Blackie and Sons, Glasgow, USA.

Sherwood-Lollar, B., Frape, S.K., Weise, S.M., Fritz, P., Macko, S.A., Welhan, W.A., 1993. Abiogenic methanogenesis in crystalline rocks. Geochim. Cosmochim. Acta 57, 5087–5097.

Sherwood-Lollar, B., Westgate, T.D., Ward, J.A., Slater, G.F., Lacrampe-Coloume, G., 2002. Abiogenic formation of alkanes in the earth's crust as a minor source for global hydrocarbon reservoirs. Nature 416, 522–524.

Soave, G., 1972. Equilibrium constants from a modified Redlich–Kwong equation of state. Chem. Eng. Sci. 27, 1197–1203.

Sørensen, H., 1997. The agpaitic rocks—an overview. Min. Mag. 407, 485–498.

Sugisaki, R., Mimura, K., 1994. Mantle hydrocarbons: abiotic or biotic. Geochim. Cosmochim. Acta 58 (11), 2527–2542.

Szatmari, P., 1989. Petroleum formation by Fischer–Tropsch synthesis in plate tectonics. AAPG Bull. 73 (8), 989–998.

Thiéry, R., Vidal, J., Dubessy, J., 1994. Phase equilibria modelling applied to fluid inclusions: liquid–vapour equilibria and calculation of the molar volume in the CO_2–CH_4–N_2 system. Geochim. Cosmochim. Acta 58 (3), 1073–1082.

Tolstikhin, I.N., Marty, B., 1998. The evolution of terrestrial volatiles: a view from helium, neon, argon and nitrogen isotope modelling. Chem. Geol. 147, 27–52.

Van den Kerkhof, A.M., 1988. The system CO_2–CH_4–N_2 in fluid inclusions: theoretical modelling and geochemical applications. PhD Thesis. Free University, Amsterdam, Holland.

Van den Kerkhof, A.M., Hein, U.F., 2001. Fluid inclusion petrography. Lithos 55, 27–47.

Van den Kerkhof, A.M., Thiéry, R., 2001. Carbonic inclusions. Lithos, 49–68.

Voytov, G.I., 1992. Chemical and carbon-isotope fluctuations in free gases (gas jets) in Khibiny. Geochem. Int. 29 (1), 14–24.

Zhang, Y.G., Frantz, J.D., 1992. Hydrothermal reactions involving equilibrium between minerals and mixed volatiles: 2. Investigations of fluid properties in the CO_2–CH_4–H_2O system using synthetic fluid inclusions. Chem. Geol. 100, 51–72.